Comparison of water column [CO_{2aq}] with sedimentary alkenone-based estimates: A test of the alkenone-CO_2 proxy

Mark Pagani,[1] Katherine H. Freeman,[2] Nao Ohkouchi,[3] and Ken Caldeira[4]

Received 10 January 2002; revised 19 April 2002; accepted 27 June 2002; published 18 December 2002.

[1] The stable carbon isotopic compositions of alkenones have been used to interpret the long-term history of the partial pressure of atmospheric carbon dioxide (pCO_2). Although extensive water column and culture studies document the potential utility and limitations of this approach, to date the accuracy of pCO_2 values derived from sedimentary alkenones remains untested. For this study we establish Holocene-aged, alkenone-based CO_{2aq} estimates ($[CO_{2aq}]_{alk}$) from 20 sites along a central Pacific Ocean transect and compare them against both observed modern water column CO_{2aq} and estimated preindustrial concentrations at the depth of alkenone production at each site. Although the $[CO_{2aq}]_{alk}$ track measured water column values, they are conspicuously lower than modern values across the subtropics. This offset likely reflects the contributions of anthropogenic CO_2 in modern surface waters relative to preindustrial concentrations at the time of alkenone production. When a model-based estimate of anthropogenic CO_2 is removed from the modern observed values, a majority (84%) of $[CO_{2aq}]_{alk}$ falls within 20% of modeled preindustrial values. Consistency between the modeled and alkenone-based estimates of preindustrial CO_2 levels points to the relative accuracy of the alkenone-CO_2 method across a wide range of ocean and biogeographic regimes, provided that phosphate concentrations, at the depth of haptophyte production, are reasonably constrained. It further suggests that light-limited growth and/or active carbon uptake, if they occur, have a negligible effect on reconstructed $[CO_{2aq}]$. *INDEX TERMS:* 3022 Marine Geology and Geophysics: Marine sediments—processes and transport; 4207 Oceanography: General: Arctic and Antarctic oceanography; 9310 Information Related to Geographic Region: Antarctica; *KEYWORDS:* alkenones, $\delta^{13}C$, carbon dioxide, Pacific Ocean

Citation: Pagani, M., K. H. Freeman, N. Ohkouchi, and K. Caldeira, Comparison of water column [CO_{2aq}] with sedimentary alkenone-based estimates: A test of the alkenone-CO_2 proxy, *Paleoceanography*, *17*(4), 1069, doi:10.1029/2002PA000756, 2002.

1. Introduction

[2] The isotopic fractionation by marine algae as measured using alkenones and carbonate phases preserved in ancient sediments holds great promise toward revealing the long-term history of atmospheric CO_2 (pCO_2). Alkenones are long-chained unsaturated ketones exclusively produced by some haptophyte algae in the modern ocean [*Volkman et al.*, 1980; *Conte et al.*, 1994]. Estimates of the partial pressure of atmospheric carbon dioxide (pCO_2) derived from this biomarker are founded on records of the carbon isotopic fractionation during marine photosynthetic carbon fixation (ε_p; expressed in ‰). ε_p for marine algae is primarily a function of the concentration of aqueous CO_2 ([CO_{2aq}]), cellular growth rates [*Bidigare et al.*, 1997, 1999], and cell geometry [*Popp et al.*, 1998a]. An accumulation of field data has provided an empirical expression of ε_p values constructed from diunsaturated alkenones ($\varepsilon_{p37:2}$) as a function of surface-water [PO_4^{3-}] and [CO_{2aq}] [*Bidigare et al.*, 1997]. Consequently, calculation of CO_{2aq} values based on $\varepsilon_{p37:2}$ require estimates of ancient surface-water [PO_4^{3-}] at the depth of haptophyte production. Recently, $\varepsilon_{p37:2}$ values from oligotrophic regions of subtropical gyres were applied to document trends in Miocene (~25–5 Ma) atmospheric carbon dioxide [*Pagani et al.*, 1999a, 1999b]. These records provide evidence that pCO_2 was substantially lower (~290–180 ppmv) than previously anticipated, suggesting that changes in pCO_2 played a secondary role in forcing the climatic swings of the early Neogene.

[3] An early application of the alkenone methodology evaluated changes in Pleistocene surface water CO_2 along the equatorial Pacific [CO_{2aq}] [*Jasper et al.*, 1994]. However, interpretation of patterns of isotopic fractionation documented in this work is confounded by potentially wide variations in interglacial/glacial upwelling rates, surface water nutrient concentrations, and haptophyte growth rates which strongly influence $\varepsilon_{p37:2}$. As a consequence, subsequent research has attempted to estimate past nutrient concentrations by proxy [*Andersen et al.*, 1999] or constrain the possible range of nutrient variability by restricting site selection to relatively stable, oligotrophic environments [*Pagani et al.*, 1999a]. Although the alkenone-CO_2 proxy

[1]Department of Geology and Geophysics, Yale University, New Haven, Connecticut, USA.
[2]Department of Geosciences, The Pennsylvania State University, University Park, Pennsylvania, USA.
[3]Department of Marine Chemistry and Geochemistry, Woods Hole Oceanographic Institute, Woods Hole, Massachusetts, USA.
[4]Climate and Carbon Cycle Group, Lawrence Livermore National Laboratory, Livermore, California, USA.

Copyright 2002 by the American Geophysical Union.
0883-8305/02/2002PA000756$12.00

Table 1. Total Data[a]

Site	Latitude	Temperature, °C	$\delta^{13}C_{37:2}$	$\varepsilon_{p37:2}$, ‰ for Preindustrial Spring		$\varepsilon_{p37:2}$, ‰ for Preindustrial Autumn		PO_4^{3-}, μmol kg^{-1} for Spring		PO_4^{3-}, μmol kg^{-1} for Autumn	
				Focus	Range	Focus	Range	Focus	Range	Focus	Range
NB77	45.97°N	10.20	−22.30	na	na	10.68	10.53–10.73	na	na	1.12	1.03–1.24
NB76	43.00°N	11.20	−22.60	na	na	10.42	10.22–10.52	na	na	0.82	0.76–0.94
NB75	40.00°N	13.90	−22.90	12.14	11.44–12.14	11.08	10.98–11.39	0.51	0.51–0.51	0.52	0.25–0.62
NB74	37.50°N	14.80	−23.20	12.24	11.48–12.24	11.60	11.48–11.89	0.33	0.32–0.39	0.32	0.12–0.52
NB73	35.25°N	16.10	−22.70	na	na	11.87	11.52–11.92	na	na	0.18	0.16–0.34
NB72	33.00°N	16.70	−23.90	13.02	13.02–13.05	12.95	12.70–13.02	0.07	0.06–0.10	0.13	0.11–0.14
NB70	27.07°N	18.10	−23.10	12.37	12.34–12.58	12.58	12.34–12.68	0.15	0.15–0.27	0.11	0.07–0.21
NB69	24.00°N	21.50	−23.50	12.57	12.32–12.80	12.37	12.32–12.57	0.03	0.03–0.03	0.15	0.08–0.18
NB68	21.82°N	23.90	−24.10	13.68	13.64–13.68	13.53	13.23–13.53	0.02	0.02–0.02	0.08	0.07–0.09
NMC1	19.00°N	24.30	−21.30	11.24	10.94–11.24	11.19	11.19–11.19	0.05	0.05–0.10	0.05	0.06–0.10
NB67	15.00°N[b]	26.60	−23.10	13.75	13.60–13.75	13.75	13.70–13.75	0.13	0.13–0.14	0.32	0.18–0.42
NB66	12.90°N	26.80	−22.70	14.07	14.07–14.07	14.07	14.04–14.07	0.10	0.10–0.15	0.15	0.15–0.15
NB65	9.98°N	27.30	−22.70	13.29	13.29–13.34	13.29	12.99–13.29	0.11	0.11–0.14	0.15	0.15–0.16
NB62	3.00°N	28.30	−22.60	13.05	12.60–13.05	12.45	12.45–12.85	0.32	0.29–0.45	0.38	0.31–0.45
NB61	0°	27.90	−22.50	13.50	12.7913.60	12.91	12.84–12.94	0.55	0.34–0.64	0.35	0.28–0.40
NGC43	2.00°S	28.30	−22.30	11.82	11.82–12.32	12.02	11.92–12.53	0.49	0.24–0.57	0.33	0.19–0.40
NB60	5.00°S	27.00	−22.10	11.88	11.98–11.88	12.03	11.98–12.03	0.61	0.55–0.65	0.63	0.52–0.70
NB59	7.00°S	26.60	−22.40	12.27	12.22–12.32	12.42	12.37–12.42	0.66	0.54–0.71	0.70	0.58–0.75
NB57	12.03°S	27.50	−19.20	10.52	10.45–10.52	na	na	0.27	0.14–0.43	na	na
NB56	14.98°S	27.60	−23.00	13.66	13.55–13.81	na	na	0.28	0.11–0.46	na	na

[a] Temperatures represent the temperature during haptophyte production based on $U_{37}^{K'}$ values [*Ohkouchi et al.*, 1999a]. Haptophyte production depths, estimated by comparing $U_{37}^{K'}$ temperatures ±1°C with seasonal depth-temperature profiles collected by NOPACCS, were used to constrain all chemical variables. "Focus" values represent $[PO_4^{3-}]$ and $\varepsilon_{p37:2}$ values estimated at the depths defined by exact $U_{37}^{K'}$ temperatures, whereas "Range" values represent the maximum/minimum ranges estimated using $U_{37}^{K'}$ temperatures ±1°C; na = data not available for the given temperature.

[b] Surface 4 cm was analyzed.

represents an important empirical approach in the assessment of ancient CO_2 levels, the accuracy of pCO_2 estimates derived from sedimentary alkenones remains untested. This uncertainty is particularly acute across oligotropic regions that, because of their stability with respect to nutrient concentrations, are considered the most appropriate locations for accurate paleo-pCO_2 reconstructions [*Pagani et al.*, 1999a]. For example, on the basis of $U_{37}^{K'}$ temperatures, haptophytes appear to grow at various depths within and below the surface mixed layer [*Ohkouchi et al.*, 1999a; *Bentaleb et al.*, 1999]. In subtropical gyres production depths potentially exceed 100 m [*Ohkouchi et al.*, 1999a], raising critical questions regarding the isotopic effect of light-limited growth [*Riebesell et al.*, 2000]. Moreover, the veracity of alkenone-pCO_2 estimates rests on the assumption that intercellular CO_{2aq} fixed during photosynthesis arrives by diffusive flux. Results from chemostat culture experiments lend support, but do not prove, a photosynthetic diffusion model for *Emiliania huxleyi*, the dominant haptophyte in the modern ocean [*Popp et al.*, 1998a]. Whether or not natural haptophyte populations have the ability to increase intercellular concentrations of inorganic carbon by actively transporting bicarbonate or CO_{2aq} remains unresolved. Finally, questions regarding the postdepositional diagenetic alteration of sedimentary alkenone isotopic compositions have not been fully addressed [*Gong and Hollander*, 1999].

[4] In this study, we determined values of $\varepsilon_{p37:2}$ based on alkenones derived from surface sediments collected along a well-studied transect in the central Pacific Ocean. Carbon dioxide concentrations estimated from analyses of these sedimentary compounds provide a basis for comparison with measured modern CO_2 concentrations and with measured values that have been corrected for contributions of anthropogenic carbon. The objective is a test of the veracity of sediment alkenone-based CO_2 estimates in a wide spectrum of open-ocean environments.

2. Site Description and Sampling

[5] Heptatriaconta-15E, 22E-dien-2-ones and heptatriaconta-8E, 15E, 22E-trien-2-ones (di- and tri-unsaturated alkenones) were extracted from central Pacific Ocean surface sediments (surface 2 cm sampled except at 15.00°N; Table 1) across a 175°E from 45°N to 15°S (Figure 1). Samples were collected with a box corer during the R/V Hakurei Maru cruises in 1992/1993, frozen, and subsequently analyzed for $U_{37}^{K'}$ temperature values [*Ohkouchi et al.*, 1999a] and carbon isotopic compositions.

[6] Although alkenones were not radiometrically dated, a Holocene age is estimated [*Ohkouchi et al.*, 1999a, 1999b] on the basis of apparent sedimentation rates of red clays in the central Pacific [*Goldberg and Koide*, 1962; *Janecek and Rea*, 1985; *Yang et al.*, 1986]. *Yang et al.* [1986] carefully determined sedimentation rates (using sediments at a depth of 10–20 cm) based on ^{230}Th, $^{230}Th/^{232}Th$, and ^{231}Pa measurements. Their results indicate that the apparent sedimentation rates of red clays are generally higher than 0.4 cm kyr^{-1} and always greater than 0.2 cm kyr^{-1}. Further, the relative porosity of the uppermost surface sediments composing our samples dramatically decrease with depth, changing from a highly liquefied character to a more consolidated state. These observations support continuous and recent deposition. Further, estimates of sedimentation rates (determined from sediments with substantially lower porosities than the uppermost 4 cm), suggests that the sediments used in

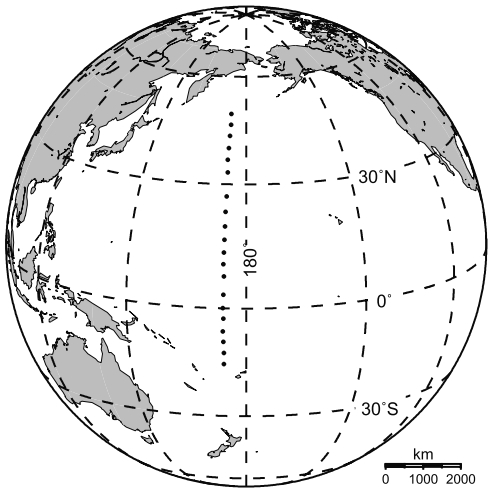

Figure 1. Site distribution.

this study largely accumulated over the past several thousand years and are not significantly influenced by chemical signatures derived from the last glaciation.

[7] Water column chemistry (including salinity, temperature, phosphate, nitrate, silica, chlorophyll, *p*H, total alkalinity, and total dissolved inorganic carbon) was measured in detail along this transect twice a year (i.e., April through June and August through September) from 1990 to 1996 under the auspices of the Northwest Pacific Carbon Cycle Study (NOPACCS); a Japanese initiative investigating the carbon cycle of the North Pacific [*Tsubota et al.*, 1999].

[8] On the basis of temperature and salinity patterns, water mass distribution is defined as sub-Arctic (48°–44°N), the Kuroshio (44°–40°N), the northern subtropics (30°–6°N), equatorial (3°N–3°S), and the southern subtropics (≥8°S) [*Harimoto et al.*, 1999].

3. Analytical Methods

[9] The determination of $U^{K'}_{37}$ values is described in detail elsewhere [*Ohkouchi et al.*, 1999a]. Briefly, wet sediments were extracted with methanol, dichloromethane/methanol (7:1, v/v), and dichloromethane/methanol (10:1, v/v) using a homogenizer and ultrasonicator. The total lipid extracts were saponified with 0.5M KOH/methanol for two hours under reflux. The neutral fraction was separated by silica gel column chromatography and the fraction containing alkenones was injected into a Carlo Erba 6000 gas chromatograph installed with an on-column injector and a HP-5 capillary column (30 m × 0.25 mm, 0.25 μm film thickness) to determine relative abundances of di- and tri-unsaturated alkenones. $U^{K'}_{37}$ temperatures are calculated using the calibration of *Prahl et al.* [1988]; $T(°C) = (U^{K'}_{37} - 0.039)/0.034$.

[10] Compound-specific isotope analyses were performed on di-unsaturated alkenones using a GC-combustion system connected to a Finnigan MAT 252 mass spectrometer [*Merritt et al.*, 1995]. Compounds eluting from a gas chromatograph are combusted over nickel and platinum at 1000°C. Water is removed through a refrigerated Nafion permeable membrane [*Leckrone and Hayes*, 1997], externally flushed with helium, and the resulting purified CO_2 is introduced into the mass spectrometer. Isotopic compositions are calculated relative to Peedee belemnite (PDB) by comparison with a gas standard calibrated to NBS-19, and assigning a value of 1.95‰ for $\delta^{13}C$ [*Ricci et al.*, 1994]: $\delta^{13}C = [(R_{SA}/R_{ST}) - 1] \times 10^3$; where R represents the $^{13}C/^{12}C$ abundance ratio, and subscripts SA and ST represent the sample and PDB standard, respectively. Analytical uncertainty determined by multiple measurements of co-injected standards is ±0.38‰.

4. Approach

[11] The degree of unsaturation of C_{37} alkenones, expressed as the unsaturation indices U^{K}_{37} and $U^{K'}_{37}$, is broadly applied in the reconstruction of past sea surface temperatures [*Sikes et al.*, 1991]. More specifically, sedimentary-derived $U^{K'}_{37}$ values likely reflect ambient water temperatures at the depth of principal alkenone synthesis. Evaluation of alkenones and mixed-layer temperatures from sediment traps in the northeast Pacific [*Prahl et al.*, 1993] and suspended particulate matter in the northwest Mediterranean Sea [*Bentaleb et al.*, 1999] illustrate the importance of subsurface haptophtye production. However, it should be noted that several factors suggest great caution is required in the application of alkenones to the reconstruction of past sea temperatures. For example, biogeographical variations in the alkenone-temperature relationship are well documented [*Sikes and Volkman*, 1993; *Rosell-Melè*, 1998; *Bentaleb et al.*, 1999]. Culture experiments demonstrate that $U^{K'}_{37}$-temperature calibrations differ for different haptophyte species and strains [*Volkman et al.*, 1995; *Conte et al.*, 1998], with nonlinear relationships at high and low temperatures for some strains [*Conte et al.*, 1998]. Further, in addition to temperature, growth status and nitrate availability can influence the degree of alkenone unsaturation [*Epstein et al.*, 1998; *Popp et al.*, 1998b; *Yamamoto et al.*, 2000].

[12] In light of these concerns, we calculate $U^{K'}_{37}$ temperatures based on a single calibration [*Prahl et al.*, 1988] derived from culture experiments of *E. huxleyi* that are genetically the same as coccolithophorids of the central Pacific [*Okada and Honjo*, 1973]. Based on measured temperature-depth profiles at each sample site (we employed the two available temperature-depth profiles published by NOPACCS: spring (April–June) and autumn (August–September)), we use $U^{K'}_{37}$ temperatures (±1°C) to estimate ranges of haptophyte production depths (Figure 2a). It is well known that seasonal changes in light, stratification, and temperature lead to regional differences in the timing of phytoplankton production. For example, *Prahl et al.* [1993] observed a seasonal flux in alkenone production in the northeast Pacific, with a clear maximum during the late spring (April to mid-June). *Winn et al.* [1995] documented a spring (May) maximum for chlorophyll *a* in the North Pacific subtropical gyre. The maximum coccolith flux in the subtropical North Atlantic occurs during the winter to early spring (January to March) [*Broerse et al.*, 2000], whereas, on the basis of $U^{K'}_{37}$

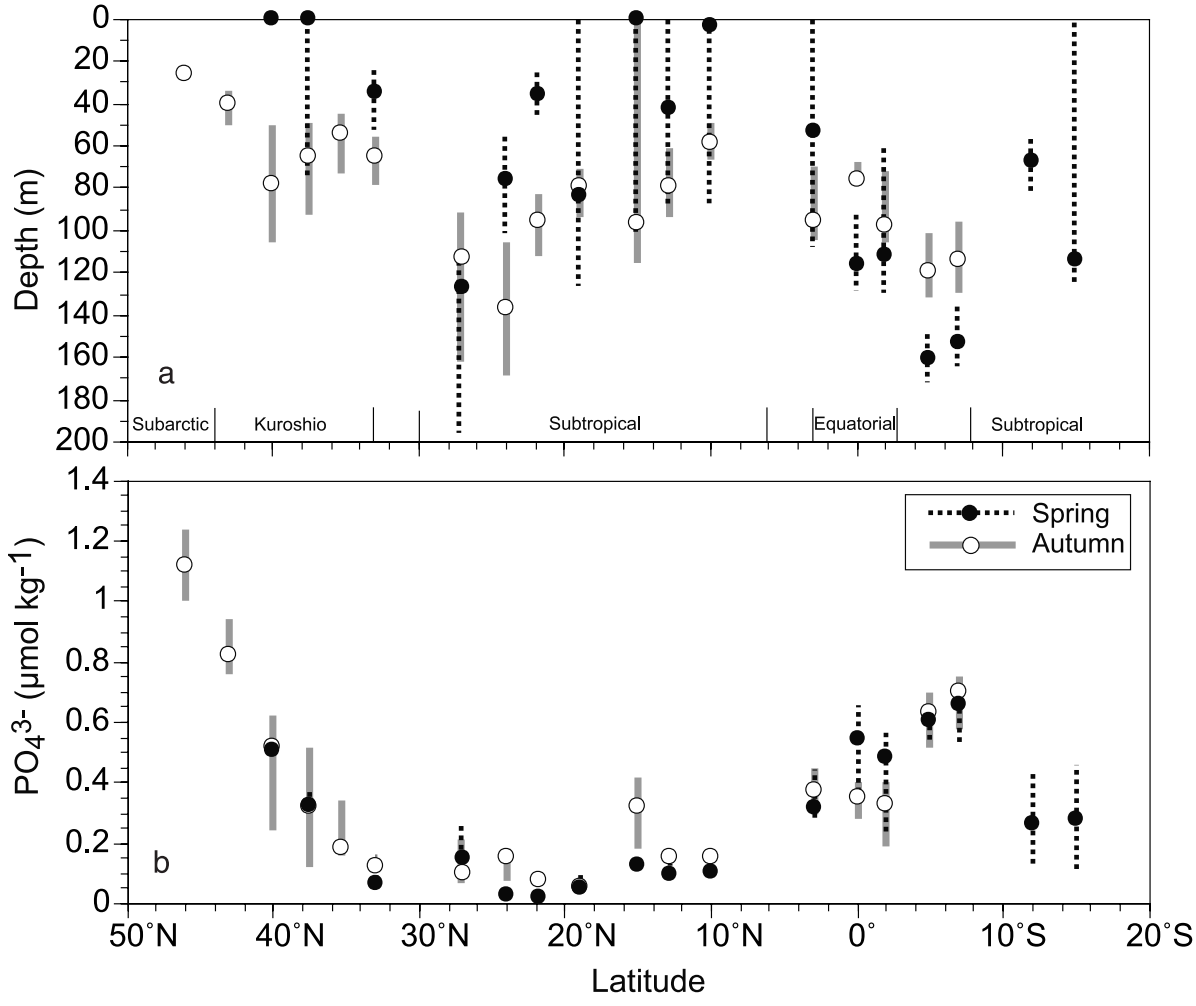

Figure 2. (a) Estimated seasonal depth of haptophyte production based on $U^{K'}_{37}$ temperature values and seasonal temperature-depth relationships established by NOPACCS. Lines represent possible range of production based on $U^{K'}_{37}$ values ±1°C; points represent depths as defined by exact $U^{K'}_{37}$ values. (b) Seasonal phosphate concentrations available for haptophyte production as defined by inferred haptophyte production depths and seasonal phosphate-depth relationships established by NOPACCS. Open circles: autumn (August and September). Closed circles: spring (April, May, and June).

temperatures, alkenone production in the northern North Pacific (48–42°N) occurs during the late summer/early fall [*Ohkouchi et al.*, 1999a; this study]. Sediment traps in the central equatorial Pacific record distinct increases in alkenone flux in November, February through March, and June to July [*Harada et al.*, 2001]. In summary, maximum alkenone production in the central Pacific likely occurs between late winter and spring for most of the locations along this transect, with important contributions from early fall production for some high latitude sites. Unfortunately, late winter water column profiles were not collected by the NOPACCS program, and thus represent a limitation for this study.

[13] Inferred haptophyte production depths are subsequently applied to constrain the probable range of $[PO_4^{3-}]$ at each site by comparing seasonal depth-phosphate profiles established by the NOPACCS program (Figure 2b; Table 1). Sedimentary alkenone-based aqueous CO_2 concentrations ($[CO_{2aq}]_{alk}$) were then calculated by applying the corresponding ranges of seasonal phosphate concentrations to calibrations of the empirical $\varepsilon_{p37:2}$-$[PO_4^{3-}]$ relationship [*Bidigare et al.*, 1997]. These alkenone-based estimates are then compared against spring and autumn records of water column $[CO_{2aq}]$ calculated from NOPACCS water column measurements ($[CO_{2aq}]_{NOPACCS}$) using a numerical model developed for CO_2 system calculations [*Lewis and Wallace*, 1998], across the range of estimated haptophyte production depths at each site.

4.1. Calculation of Alkenone-Based $[CO_{2aq}]$

[14] Alkenone CO_2 estimates are based on the expression:

$$\varepsilon_{p37:2} = \varepsilon f - b/[CO_{2aq}] \quad (1)$$

where $\varepsilon_{p37:2} = [(\delta_{CO2aq} + 1000)/(\delta_{org} + 1000) - 1]10^3$, $\delta_{org} \approx \delta^{13}C_{37:2} + 4$ [*Popp et al.*, 1998b], δ_{CO2aq} represents $\delta^{13}C$

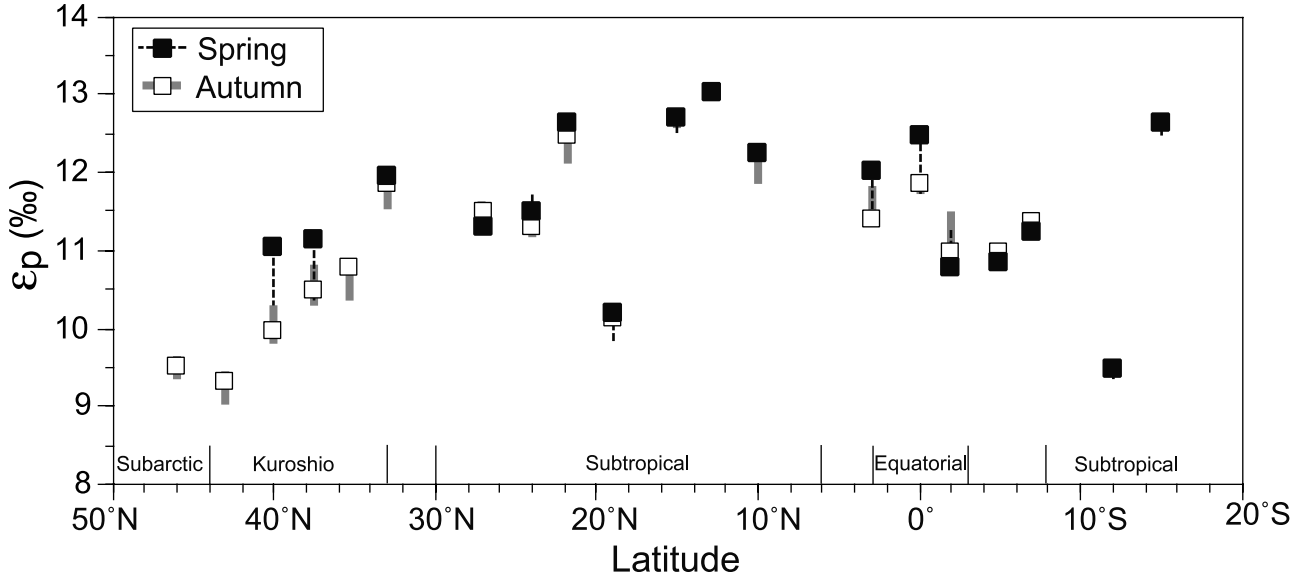

Figure 3. Values of $\varepsilon_{p37:2}$. Closed squares: $\varepsilon_{p37:2}$ values assuming spring production. Open squares: $\varepsilon_{p37:2}$ values assuming autumn production.

values of preindustrial CO_{2aq}, and b represents the sum of physiological factors, including growth rate and cell geometry, that affect total carbon isotope discrimination. Values of b are highly correlated to $[PO_4^{3-}]$ in surface waters of the modern ocean [*Bidigare et al.*, 1997]. ε_f represents the carbon isotope fractionation due to all carbon-fixing reactions. Reasonable values for ε_f range between 25–27‰ [*Popp et al.*, 1998a; *Goericke et al.*, 1994]. A variety of expressions for the physiology-dependent term b can be constructed using the range of possible values for ε_f in combination with the mathematical expressions for the geometric mean regression and 95% confidence limits from the global data set derived from all available data [*Bidigare et al.*, 1997, 1999; *Popp et al.*, 1999; *Eek et al.*, 1999; *Laws et al.*, 2001]:

$$\text{Maximum}[CO_{2aq}] = \left(4.14[PO_4^{3-}] + 125.48[PO_4^{3-}] + 107.85\right) / \left(27 - \varepsilon_p\right) \quad (2)$$

$$\text{Minimum}[CO_{2aq}] = \left(116.12[PO_4^{3-}] + 81.5\right) / \left(25 - \varepsilon_p\right) \quad (3)$$

Table 2. CO_{2aq} Values[a]

	Autumn				Spring			
Latitude	Observed CO_2	Modeled CO_2	Minimum Alkenone CO_2	Maximum Alkenone CO_2	Observed CO_2	Modeled CO_2	Minimum Alkenone CO_2	Maximum Alkenone CO_2
45.97°N	15.00	11.55	14.73	15.49	–	–	–	–
43.00°N	14.60	11.50	12.12	12.88	–	–	–	–
40.00°N	13.50	11.17	10.20	10.95	12.60	9.84	10.95	11.64
37.50°N	12.00	9.75	8.86	9.64	11.40	8.83	9.39	10.14
35.25°N	10.90		7.80	8.63	–	–	–	–
33.00°N	10.80	8.52	7.97	8.80	11.20	8.87	7.48	8.34
27.07°N	11.20	8.94	7.49	8.35	11.30	9.07	7.83	8.67
24.00°N	10.80	8.60	7.83	8.67	10.70	8.57	6.84	7.74
21.82°N	10.40	8.31	7.92	8.75	10.40	8.39	7.41	8.29
19.00°N	10.50	8.70	6.32	7.22	9.55	7.60	6.34	7.24
15.00°N	11.60	9.67	10.55	11.20	9.50	7.57	8.59	9.38
12.90°N	10.10	8.18	9.05	9.80	9.15	7.24	8.52	9.31
9.98°N	9.70	7.78	8.45	9.25	8.70	6.80	8.05	8.88
3.00°N	12.20	10.40	9.92	10.64	11.30	9.55	9.93	10.64
0.00°	9.50	7.77	10.10	10.81	12.70	11.06	12.64	13.19
2.00°S	11.20	9.55	9.23	9.99	12.00	10.38	10.50	11.22
5.00°S	13.50	11.87	11.92	12.60	12.50	10.93	11.61	12.30
7.00°S	14.00	12.37	12.94	13.56	12.70	11.08	12.42	13.07
12.03°	–	–	–	–	10.80	8.99	7.79	8.62
14.98°S	–	–	–	–	10.10	8.29	10.05	10.74

[a] Observed CO_{2aq} were calculated from NOPACCS water column measurements using a numerical model developed for CO_2 system calculations [*Lewis and Wallace*, 1998]. Modeled CO_{2aq} were calculated from observed CO_2 by subtracting anthropogenic $[CO_{2aq}]$ simulated from a modified version [*Duffy et al.*, 1998] of the Geophysical Fluid Dynamics Laboratory's Modular Ocean Model [*Pacanowski et al.*, 1991]. Maximum and minimum alkenone CO_{2aq} calculated using $\varepsilon_{p37:2}$ and PO_4^{3-} values from Table 1, and using equations (1) and (2), respectively.

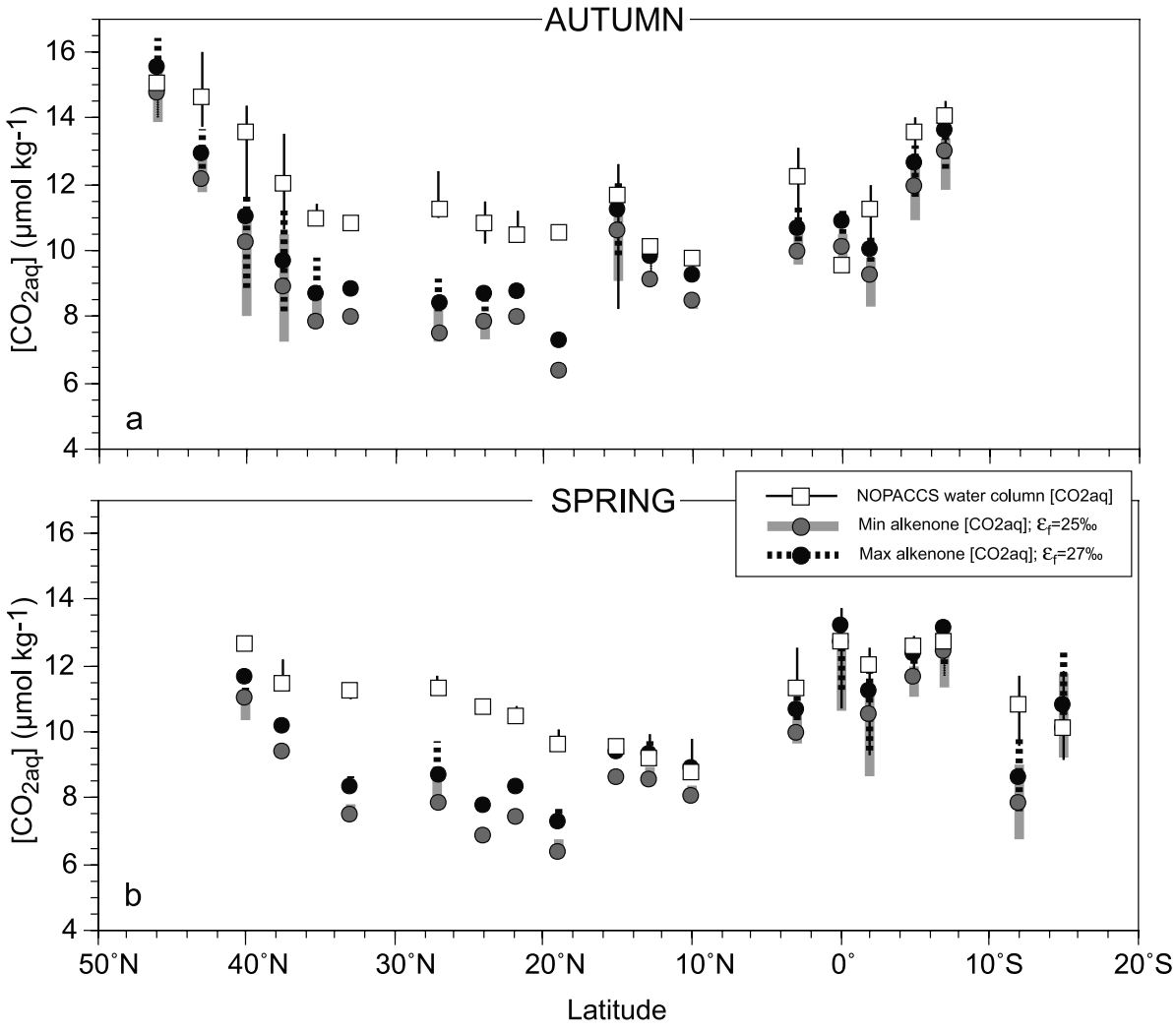

Figure 4. Comparison of alkenone-based [CO_{2aq}] with modern water column [CO_{2aq}]. (a) [CO_{2aq}] at the depth of haptophyte production assuming growth occurred during the autumn (August and September). (b) [CO_{2aq}] at the depth of haptophyte production assuming growth occurred during the spring (April, May, and June). Open squares: observed [CO_{2aq}] at the depth of haptophyte production. Closed circles: maximum alkenone-based [CO_{2aq}] calculated using an ε_f = 27‰ and the equation: [CO_{2aq}] = $(4.14[PO_4^{3-}] + 125.48[PO_4^{3-}] + 107.85)/(27 - \varepsilon_p)$. Shaded circles: minimum alkenone-based [CO_{2aq}] calculated using an ε_f = 25‰ and the equation: [CO_{2aq}] = $(116.12[PO_4^{3-}] + 81.5)/(25 - \varepsilon_p)$.

Equation (2) is based on the upper 95% confidence interval of the *b* versus $[PO_4^{3-}]$ relationship for all available data and an ε_f = 27‰. Equation (3) is based on the geometric mean regression of all available data using an ε_f = 25‰. (Note: these equations are derived from the most recent compilations of all available data, but differ only slightly from the equations used to estimate Miocene CO_2) [*Pagani et al.*, 1999a].

[15] Sediment alkenones were synthesized and deposited under preindustrial conditions. Therefore calculation of $\varepsilon_{p37:2}$ requires knowledge of the preindustrial $\delta^{13}C$ value of CO_{2aq} ($\delta^{13}C_{CO2aq}$) at the depth of haptophyte production. In general, the $\delta^{13}C$ of dissolved inorganic carbon (DIC) has been decreasing due to the combined effects of isotopic equilibration with ^{13}C-depleted anthropogenic CO_2 [*Friedli et al.*, 1986] and increased invasion of isotopically light atmospheric carbon dioxide [*Lynch-Stieglitz et al.*, 1995]. However, the rate of change of surface water $\delta^{13}C_{DIC}$, as well as the concentration of DIC, varies merdionally, with the fastest rates in the subtropical gyres and slowest at high latitudes [*Sonnerup et al.*, 1999]. For this study, upper water column $\delta^{13}C_{CO2aq}$ values were calculated from $\delta^{13}C_{DIC}$ values [*Mook et al.*, 1974] obtained by the World Ocean Circulation Experiment (WOCE P13) (P. Quay, personal communication, 2001) and *Kroopnick* [1985]. These modern $\delta^{13}C_{CO2aq}$ values were then converted to preindustrial $\delta^{13}C_{CO2aq}$ values by applying model results for the Pacific Ocean which indicate that the change in $\delta^{13}C_{DIC}$ from preindustrial times to 1990 varied across the transect [*Lynch-Stieglitz et al.*, 1995]. Preindustrial δ_{CO2aq} values were established by adjusting modern δ_{CO2aq} values by ~0.6‰ between 0° and 10° (N and S); ~0.7 to 0.8‰

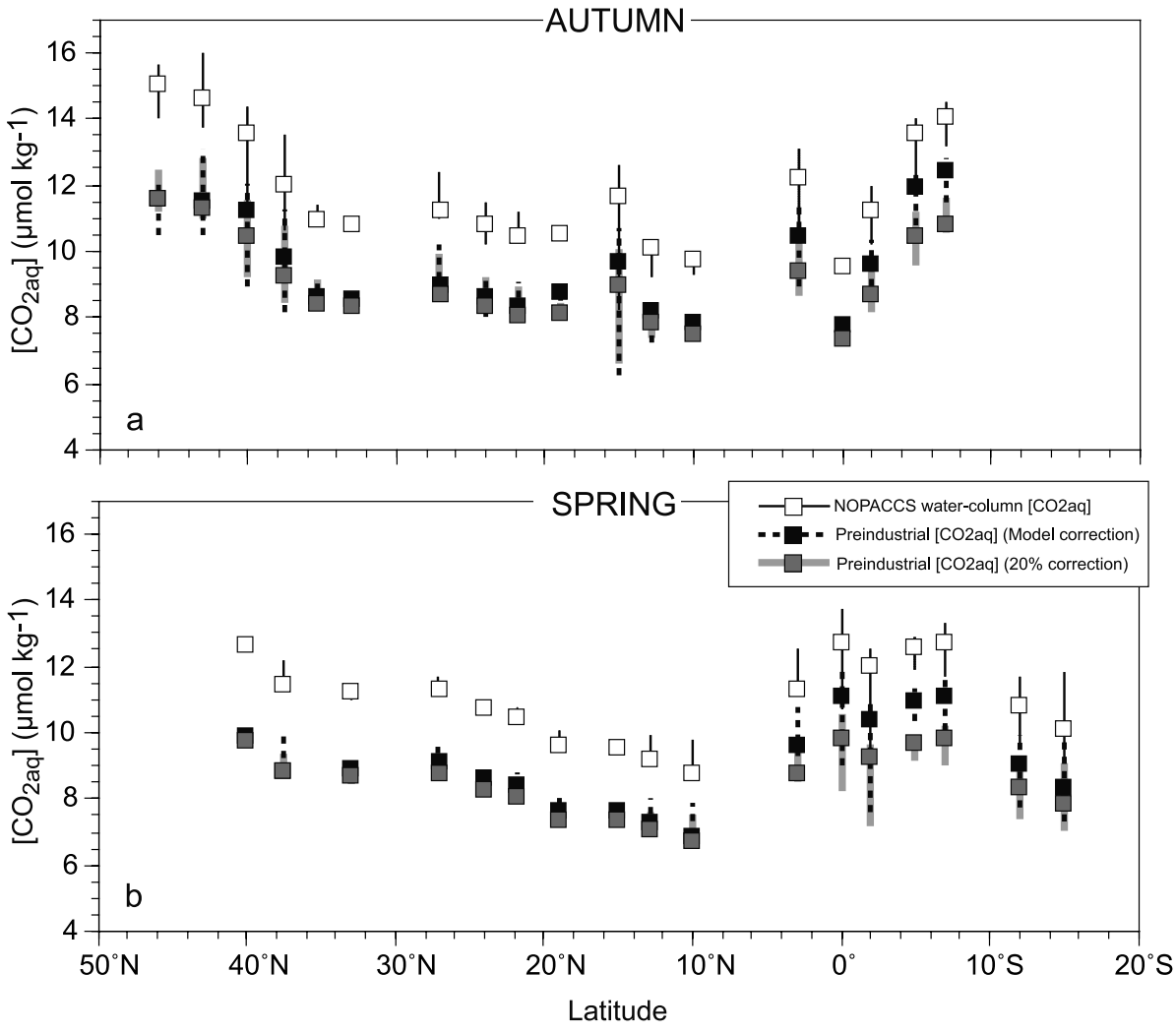

Figure 5. Comparison of measured, water column [CO_{2aq}] with estimated preindustrial water column [CO_{2aq}]. (a) Assuming autumn production (August and September). (b) Assuming spring production (April, May, and June). Open squares; modern [CO_{2aq}] at the depth of haptophyte production calculated using seasonally based NOPACCS ocean data and using a numerical model developed for CO_2 system calculations [*Lewis and Wallace*, 1998]. Shaded squares: preindustrial water column [CO_{2aq}] estimated by reducing modern water column [CO_{2aq}] by 20%. Closed squares: preindustrial water column [CO_{2aq}] estimated by reducing modern water column [CO_{2aq}] anthropogenic contributions determined using the Geophysical Fluid Dynamics Laboratory's Modular Ocean Model.

between 10° and 20°N; ~1‰ between 20° and 40°N; and ~0.7 between 40° to 50°N.

5. Results and Discussion

5.1. Estimates of Alkenone Production Depths

[16] The depth of alkenone production, as reconstructed from $U^{K'}_{37}$ temperatures, suggests a wide range of potential depth habitats across the central Pacific. In general, production depths inferred from autumn temperature profiles are deeper than those established for the spring (Figure 2a), although, this relationship is reversed at the equatorial- and low southern latitudes. Further, production depths in the low latitudes appear to occur well below the mixed layer.

[17] However, deep haptophyte production in this region is at odds with measurements of the coccolithophorid standing crop which indicate maximum concentrations at ~50 m [*Okada and Honjo*, 1973]. This discrepancy is likely the result of regional differences in the $U^{K'}_{37}$-temperature calibration. Specifically, *Okada and Honjo* [1973] document a shift in the dominance of alkenone-producing coccolithphorids from *Emiliania huxleyi* to *Gephyrocapsa oceanica* between ~5°N to 12°S. Importantly, *G. oceanica* has a different $U^{K'}_{37}$-temperature relationship [*Volkman et al.*, 1995] that returns higher temperatures relative to the *Prahl et al.* [1988] calibration for a given $U^{K'}_{37}$ value. If the *G. oceanica* calibration is applied across the low-latitude sites between 5°N and 14°S, the depth of dominant haptophyte production is limited to the autumn,

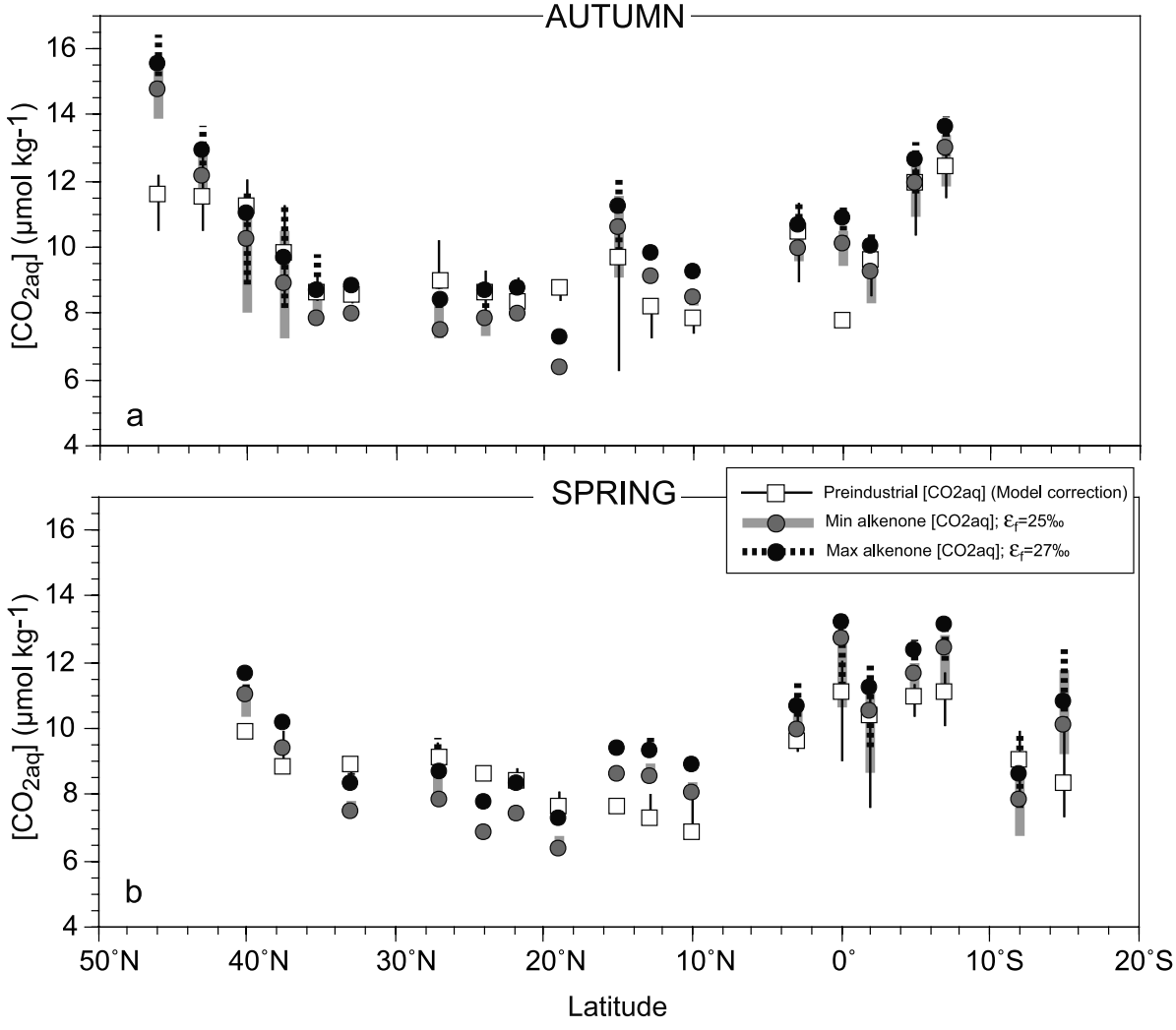

Figure 6. Comparison of alkenone-based [CO_{2aq}] with modeled preindustrial [CO_{2aq}]. (a) Assuming autumn production. (b) Assuming spring production. Open squares: preindustrial [CO_{2aq}] at the depth of haptophyte production. Closed circles: maximum alkenone-based [CO_{2aq}]. Shaded circles: minimum alkenone-based [CO_{2aq}].

predominantly within the upper mixed layer (0–50 m), and thus is compatible with the results of *Okada and Honjo* [1973].

5.2. ε_p Records

[18] From north to south, values of $\varepsilon_{p37:2}$ increase from the sub-Arctic and Kuroshio regions, reaching the highest values across the northern subtropics, and then decrease across the equatorial latitudes. South of the equatorial region $\varepsilon_{p37:2}$ values increase into the subtropics (Table 1; Figure 3).

[19] The pattern of $\varepsilon_{p37:2}$ displays a distinctive "bell-shaped" trend across the transect, with lower values associated with high- and low latitude sites characterized by upwelling. As described in equation 1, the value of ε_p increases with increasing CO_2 and decreases with increasing PO_4^{3-}. Measurements of CO_2 fugacity (fCO_2) along the transect indicate that fCO_2 remains elevated in the spring and summer across the equatorial region. In the sub-Arctic and Kuroshio regions, fCO_2 is high but subject to strong seasonal variations [*Watai et al.*, 1999]. Nutrient concentrations remain notably in the high-latitudes during both the spring and summer (Figure 2b). If elevated CO_2 concentrations were responsible for the expression of ε_p across the sites subjected to upwelling, then higher ε_p values would be predicted in these regions relative to the subtropics. However, lower ε_p values characterize upwelling regions, not higher. Therefore it appears that the relative magnitude of $\varepsilon_{p37:2}$ across the transect is primarily a function of phosphate concentration, and by extension, with cellular growth rates.

5.3. CO_2 Reconstructions and Comparisons

[20] Our estimates of dissolved CO_2 based on alkenones ($[CO_{2aq}]_{alk}$) track modern water column trends based on NOPACCS measurements ($[CO_{2aq}]_{NOPACCS}$) with the largest deviations between reconstructed and observed values across the subtropics (between 30°N and 6°N) (Table 2;

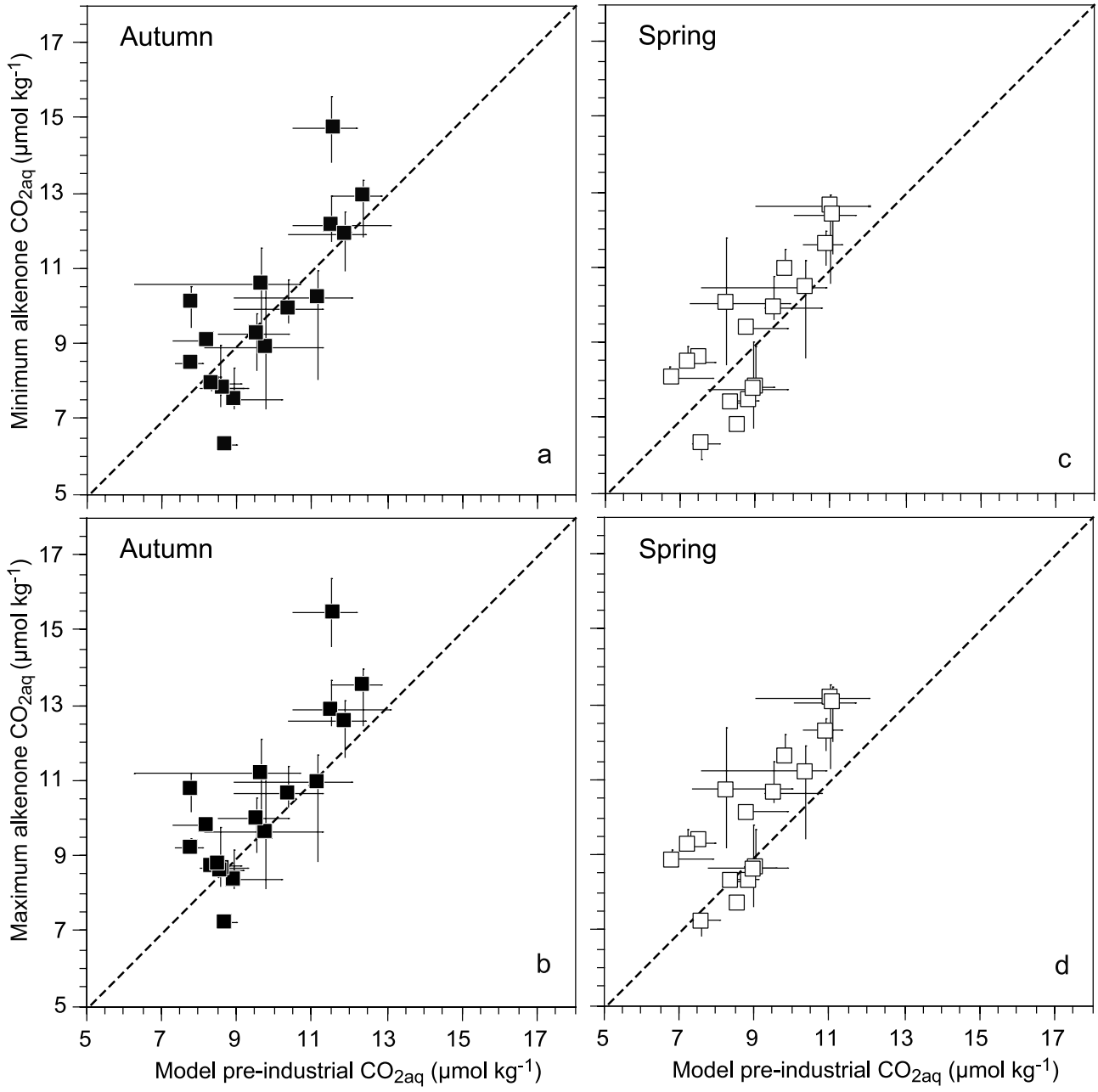

Figure 7. Modeled preindustrial [CO_{2aq}] versus alkenone-based [CO_{2aq}]. (a and b) Cross-plot of modeled preindustrial [CO_{2aq}] versus minimum and maximum alkenone-based [CO_{2aq}], respectively. Autumn production assumed. (c and d) Cross-plot of modeled preindustrial [CO_{2aq}] versus minimum and maximum alkenone-based [CO_{2aq}], respectively. Spring production assumed. Dashed line represents a 1:1 correlation.

Figure 4). The magnitude of offset between preindustrial $[CO_{2aq}]_{alk}$ and modern $[CO_{2aq}]_{NOPACCS}$ is consistent with an approximately 30% increase in pCO_2 over the past 150 years. The smallest offsets are observed across the higher latitudes, consistent with expectations, since in regions subjected to intense seasonal upwelling, a component of surface CO_{2aq} derives from deeper, preindustrial waters. The offset is greater across well-stratified waters in the subtropical latitudes, which track the rise in anthropogenic CO_2 more closely (Figure 4).

[21] Accurate comparisons between surface water CO_{2aq} concentrations and alkenone-based $[CO_{2aq}]_{alk}$ require a correction in $[CO_{2aq}]_{NOPACCS}$ in order to account for the anthropogenic rise in CO_2. While some numerical models assume that the increase in surface water dissolved CO_2 concentration has kept pace with the atmospheric increase [*Tans et al.*, 1993; *Takahashi et al.*, 1997], this assumption is most appropriate across subtropical latitudes where the upper water column is strongly stratified. In contrast, and as noted above, both low- and high latitudes are subject to intense

Table 3. Comparison of Alkenone-Based [CO_{2aq}] Reconstructions and Modeled Preindustrial [CO_{2aq}][a]

		Entire Transect				Subtropics (33°–6°N)			
		Autumn		Spring		Autumn		Spring	
Percent Deviation	Total Data, %	Minimum CO_{2alk}, %	Maximum CO_{2alk}, %	Minimum CO_{2alk}, %	Maximum CO_{2alk}, %	Minimum CO_{2alk}, %	Maximum CO_{2alk}, %	Minimum CO_{2alk}, %	Maximum O_{2alk}, %
0–5	27	33	44	12	24	13	38	0	38
0–10	49	72	61	24	41	63	50	0	63
0–15	66	78	67	65	59	75	50	38	63
0–20	84	83	89	94	76	88	100	100	63
0–25	89	83	89	100	82	88	–	–	75
0–30	96	100	89	–	94	100	–	–	88
0–35	99	–	94	–	100	–	–	–	100
0–40	100	–	100	–	–	–	–	–	–

[a] "Percent Deviation" represents the difference between alkenone-based [CO_{2aq}] reconstructions from modeled preindustrial [CO_{2aq}] in terms of percentage from preindustrial values. "Total Data" represents the percentage of total data (the sum of maximum and minimum values for spring and autumn) falling within a particular percent deviation. "Minimum CO_{2alk}" and "Maximum CO_{2alk}" represent the percentage of minimum and maximum alkenone-based [CO_{2aq}] falling within a particular percent deviation for a given season and site distribution.

seasonal upwelling which tends to "reset" surface CO_2 with a signature derived from older, deeper waters. In these regions, a 30% increase in anthropogenic CO_2 is likely too great.

[22] We estimated preindustrial water column [CO_{2aq}] ([CO_{2aq}]$_{preind}$) using two approaches: (1) reducing [CO_{2aq}]$_{NOPACCS}$ values by 23% of the observed value across the entire transect (a 23% decrease from the modern value is approximately equivalent to a 30% increase from preindustrial values due to inputs of anthropogenic CO_2), and (2) correcting [CO_{2aq}]$_{NOPACCS}$ at each site using anthropogenic [CO_{2aq}] simulated from a modified version [*Duffy and Caldeira*, 1997; *Caldeira and Duffy*, 1998] of the Geophysical Fluid Dynamics Laboratory's Modular Ocean Model [*Pacanowski et al.*, 1991] (Figure 5). Values of [CO_{2aq}]$_{preind}$ reconstructed from our model simulation show smaller contributions of anthropogenic CO_2 across the low latitudes relative to a simple 23% reduction of water column [CO_{2aq}] (Figure 5), conforming with expectations that surface waters influenced by upwelling are characterized by lower anthropogenic contributions. However, for the highest latitudes (i.e., >45°N), the model returns unreasonably low preindustrial [CO_{2aq}]. Although it is not clear why, comparison of simulated and observed radiocarbon (T. Brown, personal communication, 2001) and CFC concentrations [*Dutay et al.*, 2002] indicates that this version of the model has difficulty in simulating mixing and advection processes in the northernmost Pacific, which would explain these anomalous results.

[23] When modeled anthropogenic CO_2 is removed from the modern signal, [CO_{2aq}]$_{alk}$ accurately track water column [CO_{2aq}] (Table 2; Figures 6 and 7) with 84% of all alkenone-based CO_{2aq} estimates falling within 20% of modeled [CO_{2aq}]$_{preind}$ (Table 3). If the *G.oceanica* $U^{K'}_{37}$-temperature relationship is applied between 5°N to 12°S, correspondence between the resulting [CO_{2aq}]$_{alk}$ (based on autumn temperatures) and modeled [CO_{2aq}]$_{preind}$ improves slightly while absolute CO_{2aq} concentrations decrease ~2 to 5 μmol kg^{-1}.

[24] The relative accuracy of the alkenone-CO_2 method across a wide range of environmental conditions and production depths suggests that either the occurrence of light-limited growth and/or active carbon uptake, if they occur, have a negligible influence on reconstructed CO_{2aq} concentrations. These results demonstrate that the alkenone approach can resolve relatively small differences in water column CO_2 when phosphate concentrations are well constrained. The 15–20% offset (Table 3) represents the combined uncertainties for the alkenone proxy method, as well as averaging of haptophyte production across multiple seasons, regional differences in the $U^{K'}_{37}$ temperature calibration, and possible entrainment of pre-Holocene alkenone signatures in our samples. Thus it represents an estimate of uncertainty for the proxy method in the modern and near-recent ocean that is probably overly conservative. For ancient reconstructions, additional uncertainties include variations in haptophyte cell geometry and changes in carbon transport mechanisms that may be triggered by low [CO_{2aq}] levels. These properties are difficult, if not impossible, to evaluate for past haptophyte populations and thus they become underlying assumptions for applications in the distant past. However, given these uncertainties, the alkenone approach represents one of the best tools available for empirical estimates of relative changes in pCO_2. This work suggests that the proxy-based approach has strong potential for yielding reconstructions of absolute changes in past CO_2 levels in the near-recent ocean and perhaps in the ancient ocean under conditions that were similar to the modern environment.

6. Conclusions

[25] The magnitude of sedimentary $\varepsilon_{p37:2}$ values across the central Pacific Ocean is predominantly controlled by regional changes in nutrient concentration and not CO_2 concentration. However, if phosphate concentrations at the depth of alkenone production are well constrained, Holocene-aged, surface sediment ε_p values can be converted to CO_{2aq} concentrations that underestimate modern water column [CO_{2aq}], but accurately reproduce modeled preindustrial [CO_{2aq}]. Therefore we conclude that the alkenone-pCO_2 proxy remains a robust approach in the reconstruction of paleo-pCO_2 when applied from oceanographic regions where [PO_4^{3-}] can be reasonably estimated and CO_{2aq} concentrations were not significantly lower than preindustrial levels.

[26] **Acknowledgments.** We would like to thank B. Popp and one anonymous reviewer for their thorough and helpful critiques. We would also like to thank Gabriel Montemurro for help in processing samples.

References

Andersen, N., P. J. Müller, G. Kirst, and R. R. Schneider,The $\delta^{13}C$ signal in $C_{37:2}$ alkenones as a proxy for reconstructing Late Quaternary PCO_2 in surface waters from the South Atlantic, in *Proxies in Paleoceanography: Examples From the South Atlantic*, edited by G. Fischer and G. Wefer, pp. 469–488, Springer-Verlag, New York, 1999.

Bentaleb, I., J. O. Grimalt, F. Vidussi, J.-C. Marty, V. Martin, M. Denis, C. Hattè, and M. Fontugne, The C_{37} alkenone record of seawater temperature during seasonal thermocline stratification, *Mar. Chem.*, *64*, 301–313, 1999.

Bidigare, R. R., et al., Consistent fractionation of ^{13}C in nature and in the laboratory: Growth-rate effects in some haptophyte algae, *Global Biogeochem. Cycles*, *11*, 279–292, 1997.

Bidigare, R. R., et al., Correction to "Consistent fractionation of ^{13}C in nature and in the laboratory: Growth-rate effects in some haptophyte algae" by Bidigare et al. 1997, *Global Biogeochem. Cycles*, *13*, 251–252, 1999.

Broerse, A. T. C., P. Ziveri, J. E. van Hinte, and S. Honjo, Coccolithophore export production, species composition, and coccolith-$CaCO_3$ fluxes in the NE Atlantic (34°N 21°W and 48°N 21°W), *Deep Sea Res., Part II*, *47*, 1877–1905, 2000.

Caldeira, K., and P. B. Duffy, Sensitivity of simulated CFC-11 distributions in a global ocean model to the treatment of salt rejected during sea-ice formation, *Geophys. Res. Lett.*, *25*, 1003–1006, 1998.

Conte, M. H., J. K. Volkman, and G. Eglinton, Lipid biomarkers of the Haptophyta, in *The Haptophyte Algae*, edited by J. C. Green and B. S. C. Leadbeater, pp. 351–377, Clarendon, Oxford, UK, 1994.

Conte, M. H., A. Thompson, D. Lesley, and R. P. Harris, Genetic and physiological influences on the alkenone/alkenonate versus growth temperature relationship in *Emiliania huxleyi* and *Gephyrocapsa oceanica*, *Geochim. Cosmochim. Acta*, *62*, 51–68, 1998.

Duffy, P. B., and K. Caldeira, Sensitivity of simulated salinity in a three-dimensional ocean model to upper ocean transport of salt from sea-ice formation, *Geophys. Res. Lett.*, *24*, 1323–1326, 1997.

Dutay, J.-C., et al., Evaluation of ocean model ventilation with CFC-11: Comparison of 13 global ocean models, *Ocean Modell.*, *4*(2), 89–120, 2002.

Eek, M. E., M. J. Whiticar, J. K. B. Bishops, and C. S. Wong, Influence of nutrients on carbon isotope fractionation by natural populations of Pymnesiophyte algae in the NE Pacific, *Deep Sea Res., Part II*, *46*, 2863–2876, 1999.

Epstein, B. L., S. D'Hondt, J. G. Quinn, J. Zhang, and P. E. Hargraves, An effect of dissolved nutrient concentrations on alkenone-based temperature estimates, *Paleoceanography*, *13*, 122–126, 1998.

Friedli, H., H. Lötscher, H. Oeschger, U. Siegenthaler, and B. Stauffer, Ice core record of the $^{13}C/^{12}C$ ratio of atmospheric CO_2 in the past two centuries, *Nature*, *324*, 237–238, 1986.

Goericke, R., J. P. Montoya, and B. Fry, Physiology of isotope fractionation in algae and cyanobacteria, in *Stable Isotopes in Ecology*, edited by K. Lajtha and B. Michener, pp. 187–221, Blackwell, Malden, Mass., 1994.

Goldberg, E. D., and M. Koide, Geochemical studies of deep sea sediments by the ionium/thorium method, *Geochim. Cosmochim. Acta*, *26*, 417–450, 1962.

Gong, C., and D. J. Hollander, Evidence for differential degradation of alkenones under contrasting bottom water oxygen condition: Implication for paleotemperature reconstruction, *Geochim. Cosmochim. Acta*, *63*, 405–411, 1999.

Harada, N., N. Handa, K. Harada, and H. Matsuoka, Alkenones and particulate fluxes in sediment traps from the central equatorial Pacific, *Deep Sea Res., Part I*, *48*, 891–907, 2001.

Harimoto, T., J. Ishizaka, and R. Tsuda, Latitudinal and vertical distributions of phytoplankton absorption spectra in the central North Pacific during spring 1994, *J. Oceanogr.*, *55*, 667–679, 1999.

Janecek, T. R., and D. K. Rea, Quaternary fluctuations in the Northern Hemisphere trade winds and westerlies, *Quat. Res.*, *24*, 150–163, 1985.

Jasper, J. P., A. C. Mix, F. G. Prahl, and J. M. Hayes, Photosynthetic fractionation of ^{13}C and concentrations of dissolved CO_2 in the central equatorial Pacific during the last 255,000 years, *Paleoceanography*, *6*, 781–798, 1994.

Kroopnick, P., The distribution of ^{13}C of ΣCO_2 in the world oceans, *Deep Sea Res.*, *32*, 57–84, 1985.

Laws, E. A., B. N. Popp, R. R. Bidigare, U. Riebesell, S. Burkhardt, and S. Wakeham, Controls on the molecular distribution and carbon isotopic composition of alkenones in certain haptophyte algae, *Geochem. Geophys. Geosyst.*, *2*, paper number 2000GC000057, 2001.

Leckrone, K. J., and J. M. Hayes, Efficiency and temperature-dependence of water removal by membrane dryers, *Anal. Chem.*, *69*, 911–918, 1997.

Lewis, E., and D. W. R. Wallace, *Program Developed for CO_2 System Calculations*, Oak Ridge Nat. Lab., U.S. Dep. of Energy, Oak Ridge, Tenn., 1998.

Lynch-Stieglitz, J., T. F. Stocker, W. S. Broecker, and R. G. Fairbanks, The influence of air-sea exchange on the isotopic composition of oceanic carbon: Observations and modeling, *Global Geochem. Cycles*, *9*, 653–665, 1995.

Merritt, D. A., K. H. Freeman, M. P. Ricci, S. S. Studley, and J. M. Hayes, Performance and optimization of a combustion interface for isotope ratio monitoring gas chromatography/mass spectrometry, *Anal. Chem.*, *67*, 2461–2473, 1995.

Mook, W. G., J. C. Bommerson, and W. H. Staberman, Carbon isotope fractionation between dissolved bicarbonate and gaseous carbon dioxide, *Earth Planet. Sci. Lett.*, *22*, 169–176, 1974.

Ohkouchi, N., K. Kawamura, H. Kawahata, and H. Okada, Depth ranges of alkenone production in the central Pacific Ocean, *Global Biogeochem. Cycles*, *13*, 695–704, 1999a.

Ohkouchi, N., K. Kawamura, and H. Kawahata, Distribution of 3- to 7-ring parent and alkylated polycyclic aromatic hydrocarbons on the deep sea floor in the Central Pacific, *Environ. Sci. Technol.*, *33*, 3086–3090, 1999b.

Okada, H., and S. Honjo, The distribution of oceanic coccolithophorids in the Pacific, *Deep Sea Res.*, *20*, 355–374, 1973.

Pacanowski, R., K. Dixon, and A. Rosati, The G.F.D.L. *Modular Ocean Model Users Guide version 1.0*, NOAA/Geophys. Fluid Dyn. Lab., Princeton, N. J., 1991.

Pagani, M., M. A. Arthur, and K. H. Freeman, The Miocene evolution of atmospheric carbon dioxide, *Paleoceanography*, *14*, 273–292, 1999a.

Pagani, M., K. H. Freeman, and M. A. Arthur, Late Miocene CO_2 concentrations and the expansion of C_4 grasses, *Science*, *285*, 876–879, 1999b.

Popp, B. N., E. A. Laws, R. R. Bidigare, J. E. Dore, K. L. Hanson, and S. G. Wakeham, Effect of phytoplankton cell geometry on carbon isotopic fractionation, *Geochim. Cosmochim. Acta*, *62*, 69–77, 1998a.

Popp, B. N., F. Kenig, S. G. Wakeham, E. A. Laws, and R. R. Bidigare, Does growth rate affect ketone unsaturation and intracellular carbon isotopic variability in *Emiliania huxleyi*?, *Paleoceanography*, *13*, 35–41, 1998b.

Popp, B. N., K. L. Hanson, J. E. Dore, R. R. Bidigare, E. A. Laws, and S. G. Wakeham, Controls on the carbon isotopic composition of phytoplankton: Paleoceanographic perspectives, in *Reconstructing Ocean History: A Window Into the Future*, edited by F. Abrantes and A. Mix, pp. 381–398, Plenum, New York, 1999.

Prahl, F. G., L. A. Muehlhausen, and D. L. Zahnle, Further evaluation of long-chain alkenones as indicators of paleoceanographic conditions, *Geochim. Cosmochim. Acta*, *52*, 2303–2310, 1988.

Prahl, F. G., R. B. Collier, J. Dymond, M. Lyle, and M. A. Sparrow, A biomarker perspective on prymnesiophyte productivity in the northeast Pacific Ocean, *Deep Sea Res.*, *40*, 2061–2076, 1993.

Ricci, M. P., D. A. Merritt, K. H. Freeman, and J. M. Hays, Acquisition and processing of data for isotope-ratio-monitoring mass spectrometry, *Org. Geochem.*, *21*, 561–571, 1994.

Riebesell, U., A. T. Revill, D. G. Holdsworth, and J. K. Volkman, The effects of varying CO_2 concentration on lipid composition and carbon isotope fractionation in *Emiliania huxleyi*, *Geochim. Cosmochim. Acta*, *64*, 4179–4192, 2000.

Rosell-Melè, A., Interhemispheric appraisal of the value of alkenone indices as temperature and salinity proxies in high-latitude locations, *Paleoceanography*, *13*, 694–703, 1998.

Sikes, E., and J. K. Volkman, Calibration of alkenone unsaturation ratios ($U^{K'}_{13}$) for paleotemperature estimation in cold polar waters, *Geochim. Cosmochim. Acta*, *57*, 1883–1889, 1993.

Sikes, E., J. W. Farrington, and L. D. Keigwin, Use of the alkenone unsaturation ratio $U^{K'}_{13}$ to determine past sea surface temperatures: Core-top SST calibrations and methodology considerations, *Earth Planet. Sci. Lett.*, *104*, 36–47, 1991.

Sonnerup, R. E., P. D. Quay, A. P. McNichol, J. L. Bullister, T. A. Westby, and H. L. Anderson, Reconstructing the oceanic ^{13}C Suess effect, *Global Biogeochem. Cycles*, *13*, 857–872, 1999.

Takahashi, T., R. A. Feely, R. F. Weiss, R. H. Wanninkhof, D. W. Chipman, S. C. Sutherland, and T. T. Takahashi, Global air-sea flux of CO_2: An estimate based on measurements of sea-air pCO_2 difference, *Proc. Natl. Acad. Sci.*, *94*, 8292–8299, 1997.

Tans, P. P., J. A. Berry, and R. F. Keeling, Oceanic $^{13}C/^{12}C$ observations: A new window on ocean CO_2 uptake, *Global Biogeochem. Cycles*, *7*, 353–368, 1993.

Tsubota, H., J. Ishizaka, A. Nishimura, and Y. W. Watanabe, Overview of NOPACCS (Northwest Pacific Carbon Cycle Study), *J. Oceanogr.*, *55*, 645–653, 1999.

Volkman, J. K., G. Eglinton, E. D. Corner, and J. R. Sargent, Novel unsaturated straight-chain C37–C39 methyl and ethyl ketones in marine sediments and a coccolithophore *Emiliania huxleyi*, in *Advances in Organic Geochemistry 1979; Proceedings of the Ninth International Meeting on Organic Geochemistry, University of Newcastle-Upon-Tyne, UK, September 1979*, edited by A. G. Douglas and J. R. Maxwell, pp. 219–227, Pergamon, New York, 1980.

Volkman, J. K., S. M. Barrett, S. I. Blackburn, and E. L. Sikes, Alkenones in Gephyrocapsa oceanica: Implications for studies of paleoclimate, *Geochim. Cosomochim. Acta*, *59*, 513–520, 1995.

Watai, T., K. Harada, K. Gotoh, S. Murayama, and T. Nakazawa, Latitudinal distribution of CO_2 fugacity along 175°E in the North Pacific in 1992–1996, *J. Oceanogr.*, *55*, 655–665, 1999.

Winn, C. D., L. Campbell, J. R. Christian, R. M. Letelier, D. V. Hebel, J. E. Dore, L. Fujieki, and D. M. Karl, Seasonal variability in the phytoplankton community of the North Pacific subtropical gyre, *Global Biogeochem. Cycles*, *9*, 605–620, 1995.

Yamamoto, M., Y. Shiraiwa, and I. Inouye, Physiological responses of lipids in Emiliania huxleyi and Gephyrocapsa oceanic (Haptophyceae) to growth status and their implications for alkenone paleothermometry, *Org. Geochem.*, *31*, 799–811, 2000.

Yang, H. S., Y. Nozaki, H. Sakai, Y. Nagaya, and K. Nakamura, Natural and man-made radionuclide distributions in Northwest Pacific deep-sea sediments: Rates of sedimentation, bioturbation and ^{226}Ra migration, *Geochem. J.*, *20*, 29–40, 1986.

K. Caldeira, Climate and Carbon Cycle Group, Lawrence Livermore National Laboratory, Livermore, CA 94550, USA. (ekenc@LLNL.gov)

K. H. Freeman, Department of Geosciences, The Pennsylvania State University, University Park, PA 16872, USA. (kate@essc.psu.edu)

N. Ohkouchi, Department of Marine Chemistry and Geochemistry, Woods Hole Oceanographic Institute, Woods Hole, MA 02543, USA. (nohkouchi@whoi.edu)

M. Pagani, Department of Geology and Geophysics, Yale University, New Haven, CT 06520, USA. (mark.pagani@yale.edu)